Available online at www.sciencedirect.com
SCIENCE DIRECT®
Polymer 44 (2003) 5061–5066
polymer
www.elsevier.com/locate/polymer

Polymer communication

On the presence of a critical shell volume fraction leading to pseudo-pure droplet behavior in composite droplet polymer blends

Joël Reignier, Basil D. Favis*

CRASP, Department of Chemical Engineering, Ecole Polytechnique de Montréal, 2900 Edouard Montpetit CP 6079, Succ. Centre-Ville, Montréal Que., Canada H3C 3A7

Received 12 December 2002; received in revised form 23 May 2003; accepted 27 May 2003

Abstract

During melt mixing a ternary blend system comprised of a high density polyethylene matrix containing dispersed polystyrene and poly(methyl-methacrylate) spontaneously forms a composite droplet structure where the PS encapsulates the PMMA. This study demonstrates that the PS/PMMA composite droplet exhibits pure PS droplet behavior at a critical volume fraction of encapsulating phase (PS:PMMA ~ 0.6:0.4). This critical volume fraction is shown to be independent of the overall dispersed phase concentration, shell thickness or dispersed phase size. Furthermore, the effect is observed even though the PMMA is significantly more viscous than the encapsulating PS phase. Interfacial slip as well as the maintenance of a complete PS shell during deformation are proposed as being important factors related to this behavior. The blends were prepared via melt mixing using an internal mixer and the morphology was examined by electron microscopy.

Keywords: Composite droplet; Polymer; Blend

1. Introduction

In a series of previous studies [1–4] it has been unambiguously shown that a ternary blend, comprised of a PE(matrix) and dispersed PS and PMMA, spontaneously forms a composite droplet morphology. This is a blend structure, which possesses a matrix, a dispersed phase and sub-inclusions within the dispersed phase. It owes its formation to an overall decrease in the interfacial free energy of the system [1,4,5]. It has also been demonstrated [2], for materials identical to the one used in this study, that all of the PMMA in the blend is present as sub-inclusions within the PS and that this occurs within the first two minutes of melt mixing. The composite droplet morphology is of significant potential, since it is a possible route towards next generation polymer blends, where the dispersed phase itself can be controlled as a discrete polymer blend. Although, well known in emulsion science as double emulsions, the composite droplet morphology has received little attention in the polymer blends field.

In binary polymer blends it is well known that the viscosity ratio of the dispersed phase to the matrix has an important effect on phase morphology [6]. Increasing the viscosity of the dispersed phase with respect to that of the matrix results in a particle size increase. In the particular case of ternary blends with a core-shell structure for the dispersed phase, the situation is more complex. Luzinov et al. [7] demonstrated for polystyrene/styrene-butadiene rubber/polyethylene (PS/SBR/PE) ternary blends that the core size is influenced by the viscosity ratio of the core-forming polymer with respect to the shell material whereas the size of the dispersed phase is influenced by the viscosity ratio between the matrix and shell phase. Hemmati et al. [8] modified this concept and suggested that the dispersed phase size may be better predicted by using the ratio of the average viscosity of the two minor phases to matrix (T_{av}/T_{matrix}), rather than the viscosity ratio of shell component to matrix (T_{shell}/T_{matrix}). The average viscosity of the minor components in that case was calculated by means of a simple rule of mixtures. In a following work, Luzinov et al. [9] reported for 75/17/8 (wt%) polystyrene (PS)/styrene butadiene rubber (SBR)/polyolefin (PO), with different POs, that increasing the viscosity of the PO core increases the average size of both the PO and the SBR domains encapsulating them.

* Corresponding author. Tel.: +1-514-340-4711; fax: +1-514-340-4159.
E-mail address: basil.favis@polymtl.ca (B.D. Favis).

0032-3861/03/$ - see front matter © 2003 Published by Elsevier Ltd.
doi:10.1016/S0032-3861(03)00490-7

In another study, Reignier and Favis [2] observed that in HDPE/PS/PMMA ternary blends the composite droplet size was no longer influenced by the core material beyond a certain outer shell thickness. The study of the 80% HDPE/20% (PS + PMMA) with various PS/PMMA dispersed phase contents indicated that the composite droplet size first decreases as the quantity of PS increases from 0% to about 50% PS content (based on the dispersed phase) and levels off for higher PS contents at a value similar to the droplet size of the 80/20 HDPE/PS binary blend. The estimated PS shell thickness at 50% PS content is about 0.2 μm for a composite droplet diameter of 2 μm. Evidently, the composite droplet behaves in a fashion similar to a pure PS droplet, once a PS critical shell thickness of 0.2 μm is achieved, and this despite the high viscosity of the PMMA core.

Similar behavior has been observed for Newtonian fluids by Stone and Leal [10], who studied the rheology of a double emulsion where the dispersed phase has a core-shell structure. They showed that the dispersed phase behavior is governed by the shell viscosity when it exceeds the core viscosity. The striking result is that this is true even when the shell is very thin, typically in the order of 10% of the radius of the droplet.

The objective of this paper is to report on the factors influencing pseudo-pure droplet behavior in composite droplet polymer blends.

2. Experimental

2.1. Materials

Commercial HDPE, PS and PMMA were examined in this study. The high-density polyethylene was 4352 N and the polystyrene was 615 APR, both obtained from Dow. The poly(methyl-methacrylate) pellets were IRD-2 obtained from Rohm and Haas. A small amount (0.2 wt%) Irganox B225 antioxidant from Ciba-Geigy was added to the mixture to reduce the thermal oxidation of polyethylene.

Some of the properties of these homopolymers are given in Table 1. The complex viscosity and storage modulus were obtained at 53 rad/s and 200 °C, using a Bohlin constant stress rheometer. The experiments were performed in parallel-plate geometry with a gap of about 1.4 mm under a dry nitrogen atmosphere. In the region of estimated shear rate during blending, a PMMA/HDPE viscosity ratio of 4.5 and a PS/HDPE viscosity ratio of 1.1 are observed.

The interfacial tension of the various polymer pairs, as measured by the breaking thread technique [2], are 5.1, 2.4 and 8.6 for HDPE/PS, PMMA/PS and HDPE/PMMA, respectively.

2.2. Blend preparation

The mass of material added to the 30 cm^3 Brabender mixing chamber was chosen so that a constant volume of 20 cm^3 was achieved for each sample, based on the density at 200 °C. A typical blending experiment consisted of the following steps. With the mixer initially set at 200 °C and the roller blades turning at 100 rpm, the blend mixture was fed into the chamber. At this speed, the maximum shear rate in the mixing chamber is close to 53 s^{-1}. Once all the resin was added, the blend was allowed to mix for 8 min under a constant flow of dry nitrogen. At the end of mixing time, the mixer drive was stopped and the front plate was removed, samples were cut from the mass and dropped directly into a bath of cold water, in order to freeze-in the morphology.

It should be noted that throughout the text, the blend compositions are given in terms of volume fraction. Furthermore, the maximum shear rate in the batch mixer is used to determine the viscosity ratio. This value was chosen, since most of the breakup was expected to occur in the high shear rate region. Little difference in the viscosity ratio is observed at lower shear rates.

2.3. Microscopy/image analysis

Plane surfaces were prepared for each specimen using a microtome (Leica-Jung RM 2065) equipped with a glass knife. Cryogenic microtoming using liquid nitrogen was used to reduce the degree of surface deformation.

The microtomed samples were also subjected to the appropriate chemical treatment for 48 h to selectively dissolve one of the minor phases. Cyclohexane and acetic

Table 1
Material characteristics

	M_w[a] × 10^{-3} (g/mol)	M_n[a] × 10^{-3} (g/mol)	Melt index[b] (ASTM) (g/10 min)	Density[b] (g/cm^3) at 200 °C	η^* × 10^{-3} at 53 rad/s (Pa s) and 200 °C	G' × 10^{-4} at 53 rad/s (Pa) and 200 °C
HDPE	79	24	4	0.754	0.95	2.4
PS	289.8	140.9	15	0.969	1.05	4.6
PMMA	76.5	46.8	5.5	1.0[c]	4.3	20.5

[a] Measured by GPC.
[b] Obtained from suppliers.
[c] At 230 °C.

acid were used to extract PS and PMMA respectively, at room temperature.

After coating the desired surface with a gold–palladium alloy for 14 min in pulse mode, morphological observations were carried out with a Jeol JSM 840 scanning electron microscope operated at a voltage of 10 kV. A semi-automatic method of image analysis consisting of a digitizing table and in-house software was used to measure the diameters of the dispersed phase. For each sample, more than five fields of view and 600 diameters were analyzed. These data were averaged in order to calculate a given volume-average diameter, d_v, and the average error is $\pm 10\%$. The Saltikov correction factor was applied to the diameters determined from SEM photomicrographs of microtomed surfaces to obtain the true diameter and also to account for polydispersity effects [11].

3. Results and discussion

Fig. 1 shows the dependence of the composite droplet size on the volume fraction of PS (%) at 10, 20 and 30% dispersed phase content. The characteristic shape of the curves displays an initial drop in phase size with addition of PS to the HDPE/PMMA binary blend, followed by a leveling-off at higher PS content. Two main parameters influence the value of the composite droplet particle size obtained at different levels of PS. First, since the HDPE/PS interfacial tension is lower than that for HDPE/PMMA, the PS phase plays an emulsifying effect as it situates itself at the HDPE/PMMA interface and forms a complete shell. Secondly, increasing the PS shell thickness reduces the viscosity ratio between the HDPE matrix and the composite droplet. Both of these effects serve to diminish the particle size. At all three dispersed phase contents a plateau phase size is reached where the composite droplet size is equivalent to the pure PS phase size. It is thus clear that pseudo-pure droplet behavior is observed for all three compositions. Fig. 2 shows the morphology of the 20% dispersed phase system at different levels of PS in the composite droplet. It can be seen that for the 10 and 35% PS composite droplets, a core/shell type morphology is observed. At 65% PS a core/shell and some multicore morphologies are obtained.

To better understand the role of the PS shell thickness on the composite droplet particle size, it is helpful to present the data of Fig. 1 as a function of the PS shell thickness. As presented in a previous paper [2], if we assume a core/shell morphology and that all the PS phase is situated at the HDPE/PMMA interface, the PS shell thickness, H, is given

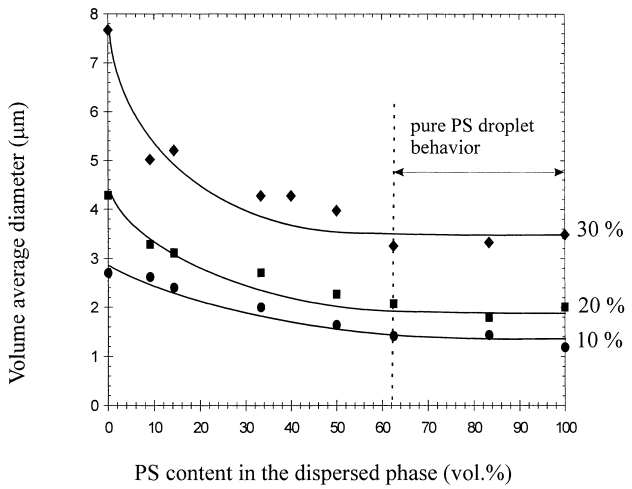

Fig. 1. Dispersed phase size as a function of PS content in the dispersed phase for HDPE/PS/PMMA ternary blends. Dispersed phase contents of 10, 20 and 30% are shown.

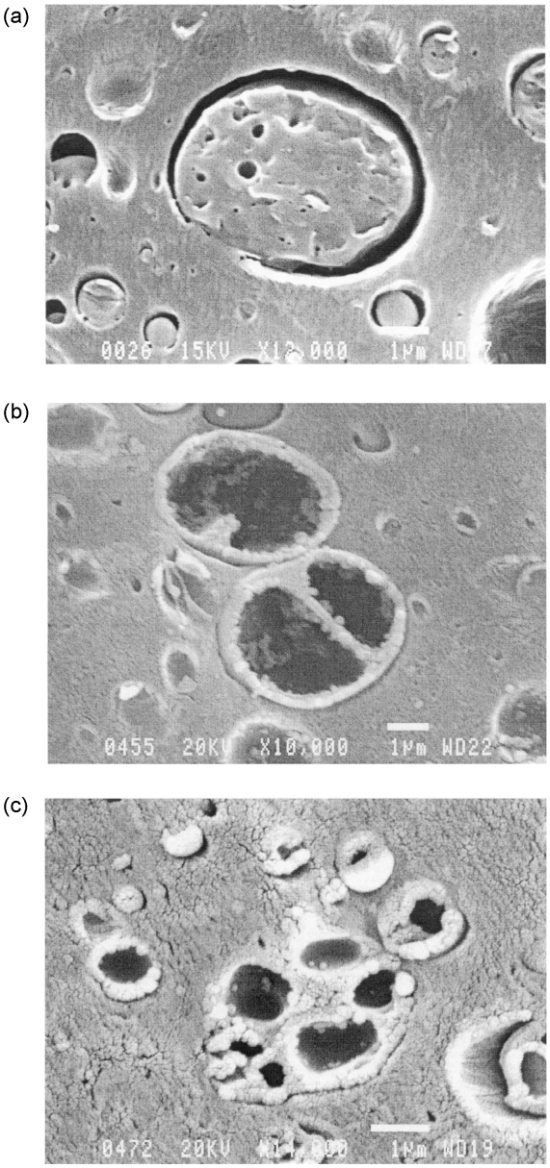

Fig. 2. Micrographs of HDPE/PS/PMMA ternary blends at different PS contents for the 20% dispersed phase system: (a) 10% PS/90% PMMA (PS extracted), (b) 35% PS/65% PMMA (PMMA extracted), (c) 62% PS/38% PMMA (PMMA extracted).

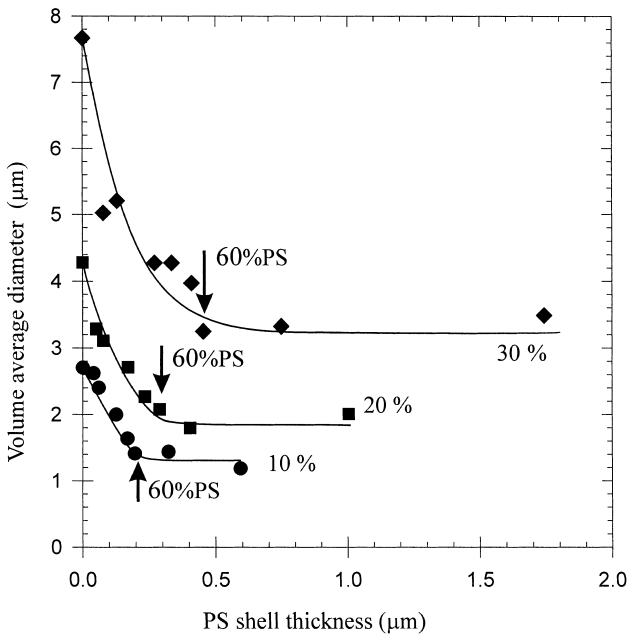

Fig. 3. Dispersed phase size as a function of PS shell thickness for HDPE/PS/PMMA ternary blends with dispersed phase contents of 10, 20 and 30%. The black arrows represent the critical PS volume fraction above which the composite droplet behaves in a similar fashion to pure PS droplet. The PS content in the composite droplet increases from left to right. The last point for each curve represents the thickness of a pure PS droplet.

by

$$H = \frac{1}{2} d_v [1 - \sqrt[3]{(1 - \phi_v)}] \quad (1)$$

where d_v is the volume average diameter of composite droplet particles and ϕ_v the volume fraction of PS (based on the dispersed phase content).

In Fig. 3, the composite droplet size is plotted as a function of the PS shell thickness. The black arrow for each curve indicates the critical PS volume fraction beyond which a particle size equivalent to pure PS dispersed phase is obtained. The results unambiguously demonstrate that at a critical composite droplet volume fraction of $\varphi_{PS} \sim 0.6$, the composite dispersed phase behaves as a droplet composed of pure shell material. Figs. 1 and 3 demonstrate that this critical volume fraction is independent of the overall dispersed phase volume percent, shell thickness or dispersed phase size. Furthermore, the effect is observed even though the PMMA is significantly more viscous than the encapsulating PS phase.

It must be pointed out that in carrying out the calculation of shell thickness in Eq. (1), one assumes that all the PS phase is situated at the HDPE/PMMA interface. However, previous work [3] indicated the presence of occluded PS inclusions in the PMMA core for the same system studied here. The presence of PS sub-inclusions in the PMMA core would tend to result in an overestimation of the shell thickness as estimated by Eq. (1) and shown in Fig. 3. Based on an evaluation of the micrographs for the 20% dispersed phase system at 9% PS volume fraction (based on the composite droplet volume), it was found that 36% of the PS was present as sub-inclusions within the PMMA. In this study, pseudo-pure composite droplet behavior is observed at PS concentrations greater than 50% based on the dispersed phase. The quantity of occluded PS in the PMMA core decreases significantly with PS concentration. An estimate of PS sub-inclusions from experimental micrographs at 62% PS/38% PMMA for the 20% dispersed phase system indicates that only 2% of PS was occluded within the PMMA. Based on the above data, the critical volume fractions indicated by the arrows in Fig. 3 can be taken as representative of the true shell volume fraction.

What are the possible physical explanations for this phenomenon?

In a blend with an HDPE matrix and a PS/PMMA core/shell composite droplet morphology, two possible slip planes exist. HDPE/PS has an interfacial tension of 5.1 mN/m and PS/PMMA has an interfacial tension of 2.4 mN/m [2]. At these molecular weights, these materials have been demonstrated to be fully immiscible and hence, very little intermixing of the phases would be expected at the interfaces. Such a material is a classic candidate to demonstrate slip at the two interfaces. These combined effects would tend to diminish the viscoelastic contribution of the PMMA core on the rheological behavior of the composite droplet as a whole.

Interfacial slip has been reported in a number of cases for immiscible polymer blends [12–14]. Utracki and Kamal [14] pointed out that blend systems which are more incompatible (large Flory–Huggins interaction parameter χ) show a larger negative deviation from additivity with respect to viscosity. Slip at the interfaces between the polymers has been proposed to explain these observations [15]. Zhao and Macosko [16] demonstrated interfacial slip for a PP/PS binary system and reported that block copolymers can suppress interfacial slip at the polymer–polymer interface. A fundamental understanding of slip at polymer melt interfaces was first proposed by Furukawa [17] and lately refined by Brochard et al. [18]. For two incompatible polymers with $\chi > 0$, there exists a diffuse interface whose width e scales as

$$e = a\chi^{-1/2} \quad (2)$$

where a is the monomer size. For example, if $\chi = 0.1$ and $a = 3$ Å, then we have $e \cong 10$ Å. Since e is much less than the radius of gyration (R_g; typically in the order of a few nm), chains are less entangled at the interface and form an interfacial region which has lower apparent viscosity than the bulk phases. A measure of the slippage at a polymer–polymer interface is given by the extrapolation length l_c [18], defined as the distance to extrapolate the velocity from the bulk phase to zero, so that

$$l_c \cong \frac{aN^3}{N_e^2} \chi^{1/2} \quad (3)$$

where N and N_e are the number of monomers per polymer chain and between entanglements, respectively, and a is the monomer size. The results in that study indicate that slippage is enhanced by large molecular weight polymer components, low entanglement molecular weights and a positive Flory–Huggins parameter. The materials used in this study fit this requirement and are many times above their entanglement molecular weight. The HDPE, PS and PMMA are about 18, 10 and 4 times above their entanglement molecular weights, respectively. They are also immiscible as mentioned earlier.

The dominance of the critical volume fraction of encapsulating phase in controlling pseudo-pure droplet behavior may be an indication that the preservation of an intact shell is also an important requirement. During melt mixing the dispersed particle can undergo significant deformation. Clearly the rupture of the external shell layer will tend to expose and hence increase the role of the PMMA core in the overall rheology of the composite droplet. In a theoretical study on the breakup of concentric double emulsion droplets in linear flows, Stone and Leal [10] suggested the possibility of breakup of the extended composite droplet if the thinning of the composite droplet occurs more rapidly than the inner droplet. In the part below we examine various scenarios of deformation of the composite droplet and comment on the expected point of rupture of the PS shell with deformation.

Fig. 4 shows the two limiting cases to be considered in this study of the influence of droplet deformation on the PS shell thickness. Note that L refers to length and B to breadth. In case I, affine deformation between the PMMA core and the PS shell is considered. In case II, we envisage that the PMMA core behaves as a rigid sphere due to the high viscosity of the PMMA phase with respect to the PS phase. Using a simple geometrical analysis, it is possible to estimate the shell thickness after deformation as a function of the L/B ratio for the 80/10/10 HDPE/PS/PMMA system (before deformation, $d_v = 2\ \mu m$ for the composite droplet diameter and $d_v = 1.6\ \mu m$ for the PMMA core size). A number of comments can be made concerning Table 2. First, if we consider that the minimum PS shell thickness has the dimension of two times the radius of gyration of the PS random coil ($R_g = 10–15$ nm) which gives a 20–30 nm minimum PS shell thickness, then the maximum deformation state is about $L/B = 100$ in case I (affine deformation). In case II (rigid PMMA domains), the breakup of the PS film about PMMA should occur for L/B values as low as 1.5. It is most likely that the composite droplet behavior in this study is closer to that of the rigid PMMA core, case II, due to the high PMMA/PS viscosity ratio ($p \cong 4$) and the likelihood of slip at the two interfaces. This could indicate that below the critical volume fraction (at lower PS contents), shell rupture is a possibility during deformation. This would tend to increase the role of the PMMA core in influencing the composite droplet size.

4. Conclusion

This study demonstrates that the PS/PMMA composite droplet exhibits pure PS droplet behavior at a critical

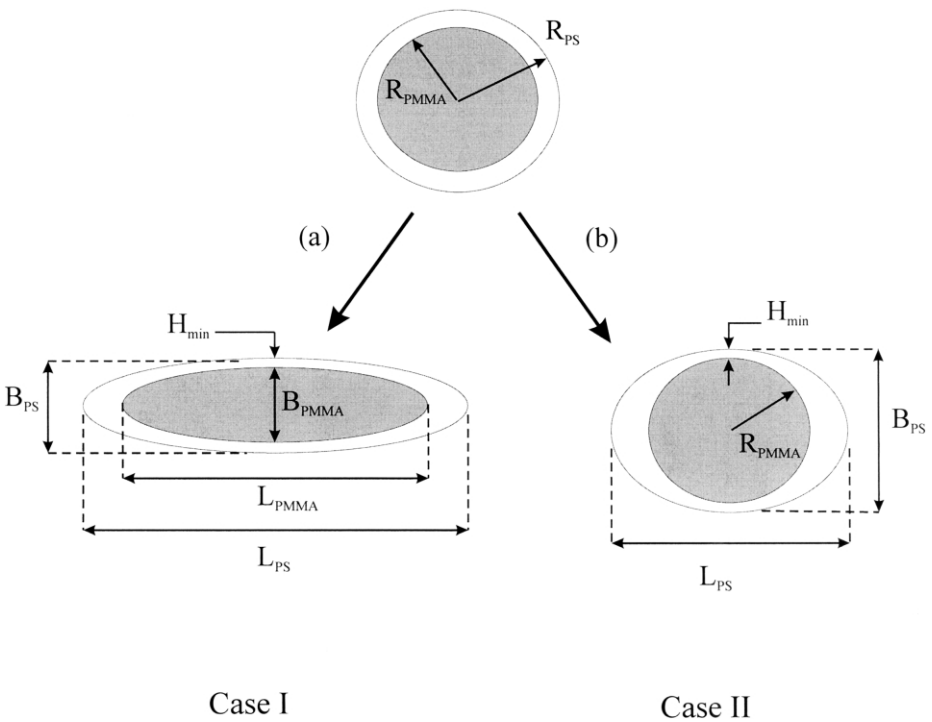

Fig. 4. Schematic representation for the deformation of the composite droplet under shear flow in two cases: (a) affine deformation between the PS/PMMA composite droplet and the PMMA core; (b) rigid PMMA core in a deformable PS shell. L refers to length and B to breadth.

Table 2
Geometrical characteristics of the dispersed phase as a function of the *L/B* ratio for the 80/10/10 (vol.%) HDPE/PS/PMMA blend system. All the dimensions are given in μm

L/B	1	1.3	1.4	1.5	2	5	10	20	100
H^{I}_{min}	0.2	0.175	0.17	0.16	0.14	0.085	0.065	0.045	0.02
H^{II}_{min}	0.2	0.075	0.045	0.015	–	–	–	–	–

volume fraction of encapsulating phase (PS:PMMA ~ 0.6:0.4). This critical volume fraction is shown to be independent of the overall dispersed phase concentration, shell thickness or dispersed phase size. Furthermore, the effect is observed even though the PMMA is significantly more viscous than the encapsulating PS phase. Interfacial slip as well as the maintenance of a complete PS shell during deformation are proposed as being important factors related to this behavior.

Acknowledgements

The authors are grateful to the Natural Science and Engineering Research Council of Canada (NSERC) for sponsoring this research. Appreciation is also extended to Dr Henry Schreiber and Dr Michel Huneault for helpful discussions.

References

[1] Guo HF, Packirisamy S, Gvozdic NV, Meier DJ. Polymer 1997;38:785.
[2] Reignier J, Favis BD. Macromolecules 2000;33:6998–7008.
[3] Reignier J, Favis BD. AIChE J 2003;49:1014.
[4] Reignier J, Favis BD, Heuzey MC. Polymer 2003;44:49.
[5] Hobbs SY, Dekkers MEJ, Watkins WH. J Mater Sci 1988;23:1219.
[6] Favis BD, Chalifoux JP. Polym Engng Sci 1987;27:1591–600.
[7] Luzinov I, Xi K, Pagnoulle C, Huynh-Ba G, Jérôme R. Polymer 1999;40:2511–20.
[8] Hemmati M, Nazokdast H, Shariat Panahi H. J Appl Polym Sci 2001;82:1129–37.
[9] Luzinov I, Pagnoulle C, Jérôme R. Polymer 2000;41:7099–109.
[10] Stone HA, Leal LG. J Fluid Mech 1990;211:123–56.
[11] Saltikov SA. The determination of the size distribution of particles in an opaque material from a measurement of the size distribution of their section, Proc second Int Cong Stereology, Helias: New York; 1967.
[12] Han CD, Yu TC. J Appl Polym Sci 1972;15:1163–80.
[13] Shi CK. Polym Engng Sci 1976;16(11):742–6.
[14] Utracki LA, Kamal MR. Polym Engng Sci 1982;22:96–111.
[15] Lin CC. Polym J 1978;11(3):185–92.
[16] Zhao R, Macosko CW. Mater Res Soc Symp 2000;629:FF2.1.1–FF2.1.10.
[17] Furukawa H. Phys Rev 1989;A40(11):6403–6.
[18] Brochard-Wyart F, de Gennes P-G, Troian SCR. Acad Sci (Paris) 1990;II:1169–73.